Analytica Chimica Acta 1303 (2024) 342523

Contents lists available at ScienceDirect

Analytica Chimica Acta

journal homepage: www.elsevier.com/locate/aca

Semiconducting polymer dots based L-lactate sensor by enzymatic cascade reaction system

Shuyi He, Weichao Liu, Steven Xu Wu *

Department of Chemistry, University of South Dakota, Vermillion, SD, 57069, United States

HIGHLIGHTS

- A highly sensitive system for L-lactate detection was prepared based on Pdots-Pt and enzymatical amplification system.
- The detection of limit (0.18 nM) was achieved through the signal amplification and bright fluorescence from Pdot-Pt.
- The sensing performance was close to the commercial L-lactate assay kit in the diluted bovine serum and artificial serum.

GRAPHICAL ABSTRACT

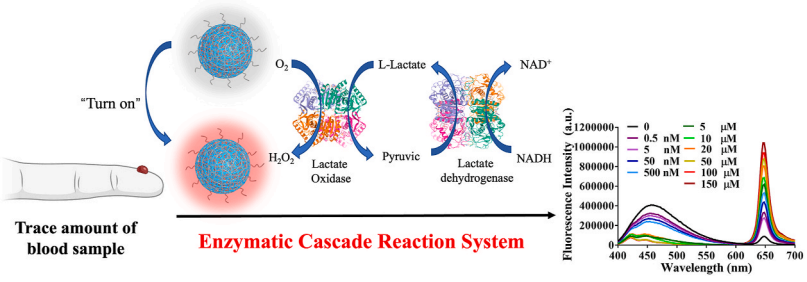

ARTICLE INFO

Handling editor: Nicola Cioffi

Keywords:
L-lactate detection
Ratiometric fluorescence
Enzymatic cascade reaction
Semiconducting polymer dots

ABSTRACT

Background: L-lactate detection is important for not only assessing exercise intensity, optimizing training regimens, and identifying the lactate threshold in athletes, but also for diagnosing conditions like L-lactateosis, monitoring tissue hypoxia, and guiding critical care decisions. Moreover, L-lactate has been utilized as a biomarker to represent the state of human health. However, the sensitivity of the present L-lactate detection technique is inadequate.

Results: Here, we reported a sensitive ratiometric fluorescent probe for L-lactate detection based on platinum octaethylporphyrin (PtOEP) doped semiconducting polymer dots (Pdots-Pt) with enzymatic cascade reaction. With the help of an enzyme cascade reaction, the L-lactate was continuously oxidized to pyruvic and then reduced back to L-lactate for the next cycle. During this process, oxygen and NADH were continuously consumed, which increased the red fluorescence of Pdots-Pt that responded to the changes of oxygen concentration and decreased the blue fluorescence of NADH at the same time. By comparing the fluorescence intensities at these two different wavelengths, the concentration of L-lactate was accurately measured. With the optimal conditions, the probes showed two linear detection ranges from 0.5 nM to 5.0 μM and 5.0 μM–50.0 μM for L-lactate detection. The limit of detection was calculated to be 0.18 nM by 3σ/slope method. Finally, the method shows good detection performance of L-lactate in both bovine serum and artificial serum samples, indicating its potential usage for the selective analysis of L-lactate for health monitoring and disease diagnosis.

Significance: The successful application of the sensing system in the complex biological sample (bovine serum and artificial serum samples) demonstrated that this method could be used for sensitive L-lactate detection in

* Corresponding author.
E-mail address: steven.wu01@usd.edu (S.X. Wu).

https://doi.org/10.1016/j.aca.2024.342523
Received 24 October 2023; Received in revised form 18 February 2024; Accepted 22 March 2024
Available online 23 March 2024

practical clinical applications. This detection system provided an extremely low detection limit, which was several orders of magnitude lower than methods proposed in other literatures.

1. Introduction

With increasing attention to health, people begin to pursue more convenient and sensitive detection methods to monitor various health indicators. L-lactate is an important biomarker formed during the anaerobic metabolism of glucose [1]. Since an excessive amount of L-lactate can be formed in the tissue when a pathological condition is present, the hyperlactatemia lasts longer, causing poor prognosis for patients of serious infections (such as sepsis). Therefore, dynamic measurement of L-lactate level is important for assessing the severity of a patient's condition and predicting the likelihood of shock, collapse, and death [2]. Studies also showed that lactate could reflect various disease states, such as cardiovascular disease, diabetes, and L-lactateosis caused by tissue hypoxia [3,4]. In addition, muscles would prefer to use anaerobic respiration to maintain energy during exercise which resulted in the accumulation of lactate in the blood. This might decrease the pH of the blood, which might lead to metabolic disturbances and muscle fatigue [5]. Therefore, monitoring lactate level is critical to master training status and health management.

The determination of lactate is usually by UV–Vis spectrophotometry in a blood sample which is normally around 0.5–1.7 mmol L^{-1} at rest and can rise to over 20 mmol L^{-1} during strenuous exercise [6]. However, this method is not specific and has low sensitivity [7]. Other technology, such as gas chromatography, capillary electrophoresis, Raman scattering-based and liquid chromatography, could be used to detect lactate reliably and quickly [8–12]. For example, Golparvar et al. have showed precise multimodal monitoring of lactate and urea levels in sweat using soft epidermal optofluidics coupled with single-band Raman scattering [12]. Madden et al. prepared electrochemical sensor based on laser-scribed graphitic carbon modified with platinum, chitosan and lactate oxidase to detect the lactate [13]. But the high cost and the need of well-trained personnel for measurements are limitations of these methods. Furthermore, the complexity of collecting blood samples and the high demands on a hygienic environment have led scientists to focus on noninvasive urine and sweat samples [14–16]. Therefore, it is essential to develop new, more sensitive, and easy to operate methods, to better assess the L-lactate level in the plasma, urine or sweat sample.

Ratiometric fluorescence is a technique that provides precise and quantitative analysis, which has received extensive attention and has been applied to the detection of lactate [17]. Its advantages include high sensitivity, reliability, short response time, low cost and simple operation [18]. Ratiometric fluorescence sensors typically use two (or more) fluorescent materials with different emission wavelengths as output signals [19]. Through self-calibration, the influence of external factors on detection results can be avoided, which would improve the sensitivity and accuracy of detection method [20]. A variety of ratiometric fluorescence probes have been developed for sensing, imaging, and biomedical applications [21–24]. This inspired us to design an ultrasensitive ratiometric fluorescence-based method for the detection of lactate.

Semiconducting polymer dots (Pdots) have attracted great interest as fluorescent probes because of their unique advantages in fluorescence and chemical properties [25–27]. Pdots have the advantages of high quantum yield, strong brightness, good optical stability and biocompatibility, which have been widely used in the field of biomedicine [28–31]. The high quantum yield of Pdots provided a bright fluorescence intensity under the same excitation condition, which will ensure the high sensitivity of the probe for bioimaging and biosensors, allowing for clearer images and more precise signal read-out. Furthermore, Pdots have been used for the fabrication of ratiometric fluorescent sensors based on their own fluorescence and utilization of FRET between Pdots and other dyes. For example, Changfeng Wu has used PtOEP doped Pdots for the detection of oxygen level in cells, which showed very bright phosphorescence and proportional emission that can be sensed in single particles and have the potential to quantitatively image local molecular oxygen concentrations in living cells and tissues [32]. In order to improve the sensitivity of the method, a step of signal amplification process may be easily incorporated into the sensor. Enzymatic cascade reactions are regarded as an excellent method to amplify the detection signal [33,34]. For example, Sun's group proposed a glucose transducer by combining glucose oxidase and catalase onto polymer dots, hydrogen peroxide produced during glucose oxidation can be rapidly decomposed, preventing its accumulation and improving the sensor's photostability, enzymatic activity and biocompatibility. This enzyme cascade reaction system improves the long-term stability of polymer dot glucose sensors, leading to better continuous glucose monitoring [35].

In this work, we reported an ultra-sensitive platform based on Pdots-Pt for the detection of trace amount of L-lactate by coupling with enzymatic cascade reaction (Scheme 1). The sensing system employed Pdots-Pt as signal transducer and enzymatic cascade reaction to selectively recognize lactate and amplify the signal. Pdots-Pt were composed of platinum octaethylporphyrin (PtOEP), which was sensitive to changes in oxygen concentration, and poly(9,9′-*n*-dihexyl fluorene) (PDHF), which was a fluorescent semiconducting polymer insensitive to oxygen. Without lactate, the system showed strong blue fluorescence due to the presence of large amount of NADH and weak red fluorescence from Pdots-Pt with the irradiation of 370 nm light. In the presence of lactate, O_2 and NADH in the system were continuously consumed by the lactate oxidation and pyruvate reduction through the enzymatic cascade reaction, which resulted in the enhancement of the red fluorescence intensity from Pdots-Pt and the decline of the blue fluorescence intensity from the NADH. With the optimal reaction conditions, the method achieved a detection of limit of 0.18 nM for the lactate with two linear ranges from 0.5 nM to 5.0 μM and 5.0 μM–50.0 μM.

2. Experimental section

2.1. Materials and instruments

The tetrahydrofuran (THF), platinum octaethylporphyrin (PtOEP), poly(9,9-di-*n*-hexylfluorenyl-2,7-diyl) (PDHF), poly(styrene-*co*-maleic anhydride) (PSMA), lactate dehydrogenase (LDH), N-(2-hydroxyethyl) piperazine-N'-(2-ethanesulfonic acid) (HEPES), β-Nicotinamide adenine dinucleotide, reduced disodium salt hydrate (NADH), L-lactate, pyruvic acid, uric acid, glucose, lactose, fructose, ascorbic acid, citric acid, acetaminophen, cysteine, arginine, glycine, were purchased from Sigma-Aldrich Corporation (USA). The lactate oxidase (Lox) was purchased from TOYOBO incorporated (TOYOBO, USA). Fetal bovine serum (FBS) was purchased from Gibco Life Technologies (USA). Water used to prepare all solutions was purified using Milli-Q System (18.2 MΩ cm, Millipore Ltd., USA). Fluorescence emission spectra were recorded on a FluoroMax spectrofluorometer (HORIBA Scientific Co., Japan).

2.2. Preparation of Pdots-Pt

The Pdots-Pt was synthesized based on a nano-precipitation method. Briefly, 0.1 mL of PDHF (1 mg mL^{-1}), 0.01 mL of PtOEP (1 mg mL^{-1}) and 0.01 mL of PSMA (1 mg mL^{-1}) were dissolved in 0.88 mL of THF. Then the solution was quickly injected into 5.0 mL of water under ultrasonication for 1 min. Pdots-Pt was formed and the organic solvent THF was removed by evaporation at 90 °C for 20 min blowing with

nitrogen.

2.3. Characterization of Pdots-Pt

The size and morphology of Pdots-Pt were measured by a transmission electron microscope (Tecnai G2 F30, FEI, USA). The size distribution of nanoparticles was determined by a Zetasizer Nano ZS dynamic light scattering (Malvern, UK). The absorption spectrum was obtained by GENESYS 30 visible spectrophotometer (Thermo Scientific, USA). Fluorescence experiments were performed using a Fluoromax Spectrofluorometer (Horiba, USA).

2.4. Fluorescence measurement

A 1000 μL aliquot of the sample was held in a disposable cuvette. The fluorescence spectrum was recorded between 400 nm and 700 nm by exciting at 370 nm. Both excitation and emission slits were set at 2 nm. The experimental data was analyzed using the software GraphPad Prism 6 (GraphPad, LaJolla, CA).

2.5. Feasibility of the sensor for lactate detection

A 5.0 μL aliquot of 100 mM L-lactate was added in a 995.0 μL reaction buffer (2.0 mg L^{-1} Pdots-Pt, 0.5 mM NADH, 7 U mL^{-1} Lox, 32 U mL^{-1} LDH, and 10 mM HEPES, pH 7.5). Afterwards, 700.0 μL hexane were added for liquid seal. The mixture was incubated at room temperature for 50 min. The fluorescence spectra were measured with an excitation wavelength of 370 nm. Then, the optimization of the concentrations of NADH, Pdots-Pt, Lox, and LDH, reaction time, and pH were conducted by measuring the fluorescence enhancement of the system.

2.6. Optimization of the sensor for lactate detection

For optimization of NADH concentration, a 5.0 μL aliquot of 100 mM L-lactate was added in a 995.0 μL reaction buffer (2.0 mg L^{-1} Pdots-Pt, different concentation of NADH (0.0 mM,0.1 mM,0.2 mM,0.3 mM, 0.4 mM, 0.5 mM), 7 U mL^{-1} Lox, 32 U mL^{-1} LDH, and 10 mM HEPES, pH 7.5). Afterwards, 700.0 μL hexane were added for liquid seal. The mixture was incubated at room temperature for 50 min. The fluorescence spectra were measured with an excitation wavelength of 370 nm. For optimization of Pdots concentration, a 5.0 μL aliquot of 100 mM L-lactate was added in a 995.0 μL reaction buffer (different concentation of Pdots-Pt (0 mg L^{-1}, 1 mg L^{-1}, 2 mg L^{-1}, 3 mg L^{-1}, 4 mg L^{-1}, 5 mg L^{-1}, 10 mg L^{-1}, and 15 mg L^{-1}), 0.5 mM NADH, 7 U mL^{-1} Lox, 32 U mL^{-1} LDH, and 10 mM HEPES, pH 7.5). Afterwards, 700.0 μL hexane were added for liquid seal. The mixture was incubated at room temperature for 50 min. The fluorescence spectra were measured with an excitation wavelength of 370 nm. For optimization of incubation time, a 5.0 μL aliquot of 100 mM L-lactate was added in a 995.0 μL reaction buffer (2.0 mg L^{-1} Pdots-Pt, 0.5 mM NADH, 7 U mL^{-1} Lox, 32 U mL^{-1} LDH, and 10 mM HEPES, pH 7.5). Afterwards, 700.0 μL hexane were added for liquid seal. The mixture was incubated at room temperature for different time. The fluorescence spectra were measured with an excitation wavelength of 370 nm. For optimization of pH, a 5.0 μL aliquot of 100 mM L-lactate was added in a 995.0 μL reaction buffer (2 mg L^{-1}dots-Pt, 0.5 mM NADH, 7 U mL^{-1} Lox, 32 U mL^{-1} LDH, and 10 mM different pH of HEPES (pH 5.5, pH 6.5, pH 7.5, pH 8.5, pH 9.5). Also, a 5.0 μL aliquot of 100 mM DI water was added in a 995.0 μL reaction buffer (2 mg L^{-1}dots-Pt, 0.5 mM NADH, 7 U mL^{-1} Lox, 32 U mL^{-1} LDH, and 10 mM different pH of HEPES (pH 5.5, pH 6.5, pH 7.5, pH 8.5, pH 9.5). Afterwards, 700.0 μL hexane were added for liquid seal. The mixture was incubated at room temperature for 50 min. For optimization of concentration of Lox, a 5.0 μL aliquot of 100 mM L-lactate was added in a 995.0 μL reaction buffer (2 mg L^{-1}dots-Pt, 0.5 mM NADH, different concentration of Lox (0 U mL^{-1}, 1.5 U mL^{-1}, 3.5 U mL^{-1}, 7 U mL^{-1}, 10.5 U mL^{-1}, 14 U mL^{-1}, 17.5 U mL^{-1}), 32 U mL^{-1} LDH, and 10 mM HEPES pH 7.5. Afterwards, 700.0 μL hexane were added for liquid seal. The mixture was incubated at room temperature for 50 min. The fluorescence spectra were measured with an excitation wavelength of 370 nm. For optimization of concentration of LDH, a 5.0 μL aliquot of 100 mM L-lactate was added in a 995.0 μL reaction buffer (2 mg L^{-1}dots-Pt, 0.5 mM NADH, 7 U mL^{-1} Lox, different concentration of LDH Lox (0 U mL^{-1}, 16 U mL^{-1}, 24 U mL^{-1}, 32 U mL^{-1}, 40 U mL^{-1}, 48 U mL^{-1}), and 10 mM HEPES pH 7.5. Afterwards, 700.0 μL hexane were added for liquid seal. The mixture was incubated at room temperature for 50 min. The fluorescence spectra were measured with an excitation wavelength of 370 nm.

2.7. Sensitivity investigation

Under the optimized reaction conditions, the sensitivity of the sensor for lactate detection was conducted. A 5.0 μL aliquot of different concentrations of L-lactate were added in a 995.0 μL reaction buffer (5.0 mg L^{-1} Pdots-Pt, 0.4 mM NADH, 7 U mL^{-1} Lox, 32 U mL^{-1} LDH, and 10 mM HEPES, pH 7.5). Afterwards, 700.0 μL of hexane were added for liquid seal. The mixture was incubated at room temperature for 30 min. The final concentrations of L-lactate in the solution were 0, 0.0005, 0.005,

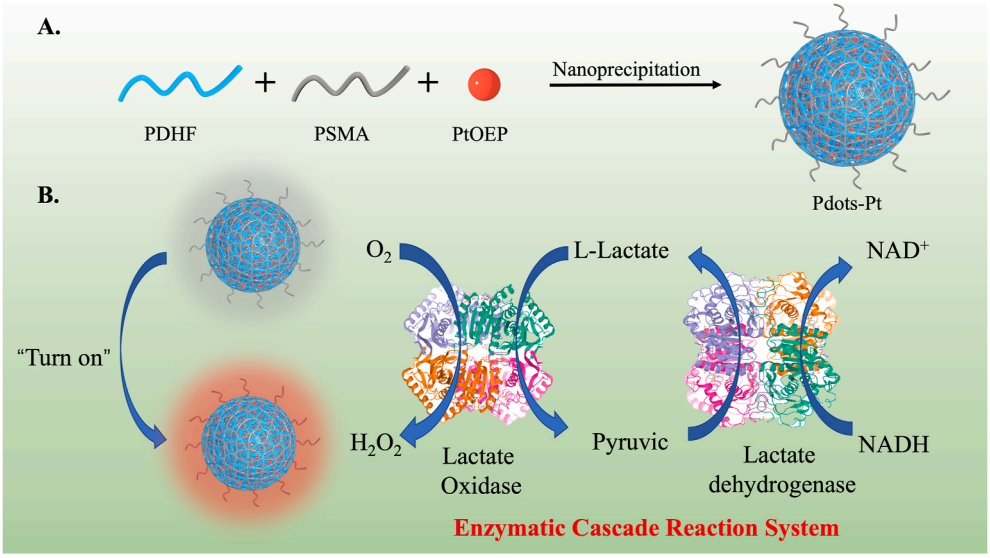

Scheme 1. Schematic illustration of lactate detection system.

0.05, 0.5, 5.0, 10.0, 20.0, 50.0, 100.0, and 150.0 μM. The fluorescence spectra of each solution were recorded with the excitation wavelength of 370 nm.

2.8. Selectivity investigation

The selectivity of the sensor over different interferences (uric acid, glucose, lactose, fructose, ascorbic acid, citric acid, the selectivity of the sensor over different interferences (uric acid, glucose, lactose, fructose, ascorbic acid, citric acid, acetaminophen, cysteine, arginine, glycine) were also investigated. A 5.0 μL aliquot of 100 mM of different interferences was added in a 990.0 μL reaction buffer (5.0 mg L^{-1} Pdots-Pt, 0.4 mM NADH, 7 U mL^{-1} Lox, 32 U mL^{-1} LDH, and 10 mM HEPES, pH 7.5) with or without a 5.0 μL aliquot of 100 mM L-lactate. Afterwards, 700.0 μL hexane were added for liquid seal. The mixture was incubated at room temperature for 30 min. The final concentrations of these interferences and lactate were 0.5 mM. Finally, the fluorescence intensity of each solution was measured.

2.9. Lactate detection in diluted fetal bovine serum

To investigate the ability of the sensor in real samples, we measured the recovery efficiency of the spiked lactate in the diluted bovine serum. The fetal bovine serum samples diluted 20 times by 10 mM HEPES buffer (pH 7.5) were first heated at 65 °C for 30 min, then centrifuged at 10,000 rpm for 10 min to extract the supernatant. The treated fetal bovine serum samples were used to prepare the determination medium (5.0 mg L^{-1} Pdots-Pt, 0.4 mM NADH, 7 U mL^{-1} Lox, 32 U mL^{-1} LDH). A 5.0 μL aliquot of different concentration of L-lactate were added in a 995.0 μL determination medium. Afterwards, 700.0 μL of hexane were added for liquid seal. The mixture was incubated at room temperature for 30 min. The final concentration of L-lactate in the solution was 0, 0.02, 0.2, 10.0, and 40.0 μM. Finally, the fluorescence intensity of each solution was measured.

3. Results and discussion

3.1. Design of the L-lactate sensor by coupling Pdots-Pt with enzymatic cascade reaction

In this work, a sensitive sensor based on enzymatic cascade reaction was reported for L-lactate detection. As shown in Scheme 1, the detection system consists of two enzymatic cascade reactions, which involved LOX, LDH, NADH, and oxygen. Pdots-Pt was used a signal transducer. Pdots-Pt was prepared by blending blue-emitting semiconducting polymer poly[(9,9-di-*n*-octylfluorenyl-2,7-diyl)-*alt*-(benzo[1–3]thiadiazol-4,8-diyl)] (PDHF) and red emitting platinum octaethylporphyrin (PtOEP). With the efficient FRET from PDHF to PtOEP, the Pdots-Pt would present the red fluorescence from PtOEP. Due to the oxygen-sensitive property of PtOEP, the Pdots-Pt showed an oxygen-dependent red fluorescence intensity. In the presence of lactate oxidase (Lox), L-lactate was oxidized to pyruvate, which consumed oxygen and generated hydrogen peroxide. As the reaction proceeded, the red fluorescence of Pdots-Pt that was originally quenched by oxygen would increase due to the consumption of oxygen. On the other hand, newly formed pyruvate was converted to L-lactate by lactate dehydrogenase (LDH). In this reaction, NADH with blue fluorescence would be continuously consumed and transformed into non-fluorescent NAD^+. As a result, the blue fluorescence from PDHF used as an internal reference, which was originally covered by a large amount of blue fluorescence of NADH, would be revealed. With this enzymatic cascade reaction, a small amount of L-lactate could continue to feed the cyclic reaction to exhaust the oxygen and NADH in the system. Therefore, the red fluorescence of Pdots-Pt would be continuously enhanced, with the continuously reduced blue color fluorescence. Within a fixed reaction time, by comparing the changes of the fluorescence intensities at two difference wavelengths, the initial L-lactate concentration would be detected through this ratiometric method.

3.2. Feasibility study

To determine the feasibility of this sensing principle, the fluorescent spectra of the sensing system at different conditions were demonstrated in Fig. 1. We first compared the fluorescence spectra of Pdots-Pt in the presence and absence of oxygen. The results from curve a and curve b in Fig. 1A showed that the Pdots-Pt in the absence of oxygen (curve b) had a significantly enhanced red fluorescence intensity at 650 nm from PtOEP compared with the Pdots-Pt in the presence of oxygen (curve a). However, the blue fluorescence from PDHF in Pdots-Pt had negatable changes. Therefore, Pdots-Pt could be used to monitor the change of oxygen level in the system using the ratio of fluorescence intensities at 650 nm–422 nm (I650/I422). In the absence of L-lactate and pyruvate, the sensor consisting of Pdots-Pt, NADH, lactate oxidase (Lox) and lactate dehydrogenase (LDH) exhibited a negligible red fluorescence intensity (~650 nm) from PtOEP and a broad blue to green fluorescence peak (~422 nm) caused by the presence of NADH (curve a), indicating that no enzymatic cascade reaction was triggered without L-lactate or pyruvate (Fig. 1B). In contrast, when pyruvate (curve b) or L-lactate (curve c) was introduced, the red fluorescence intensity was significantly enhanced and the blue to green fluorescence peak significantly decreased (curve b and c, due to the enzymatic cascade reaction triggered consumption of oxygen. The significant change of fluorescence intensity in the presence of L-lactate or pyruvate was attributed to the continuous conversion between L-lactate and pyruvate, which exhausted the oxygen and NADH in the system by enzymatic cascade reaction. These results clearly showed that the Pdots-Pt sensing platform based on enzymatic cascade reaction could be used for detection of L-lactate or pyruvate.

3.3. Characterization of Pdots-Pt

The morphological features of Pdots-Pt were displayed in Fig. 2A and B, which showed that the Pdots-Pt exhibit spherical structure and well-dispersed. As shown in Fig. 2 C, Pdots-Pt had a non-representative circular shape with a diameter of 25–30 nm by measuring the diameters of 100 nanoparticles. The SEM (Fig. S1A) images show that the sample of Pdots-Pt has uniform morphology with particle sizes ranging from 25 to 35 nm (Fig. S1B). The hydrodynamic diameter of Pdots-Pt measured by DLS displayed in Fig. 2D, indicating the uniform size distribution of hydrodynamic diameters (23.25 ± 1.92 nm). The surface zeta potentials of Pdots-Pt were about −4.33 mV, which indicated the good stability in solution.

3.4. Optimization of the lactate detection system

In order to obtain the best performance of the sensing system, a series of conditions, including the concentrations of NADH, Pdots-Pt, Lox, LDH, reaction time, and pH were optimized. First, the concentration of NADH was critical for the lactate dehydration reaction and the background signal. Excess NADH would cover the fluorescence signal of PDHF, making the blue fluorescence value as the denominator too high and the decreased sensitivity. Low concentration of NADH would cause an incomplete enzymatic cascade reaction, and the O_2 would not be consumed completely. By testing different concentration of NADH, including 0, 0.1, 0.2, 0.3, 0.4, 0.5 mM, we found that the ratio of fluorescence intensities (I650/I422) had the largest value when the 0.4 mM NADH was used (Fig. 3A). Because the ratio depends on the consumption of O_2 and NADH by the enzymatic cascade reaction, the reaction time was optimized to obtain the highest fluorescence intensity by detecting 0.5 mM lactate. As Fig. 3B showed, the control without lactate had a ratio of fluorescence intensity (I_{650}/I_{422}) nearly no change within 60 min. In the presence of 0.5 mM L-lactate, the ratio was dramatically

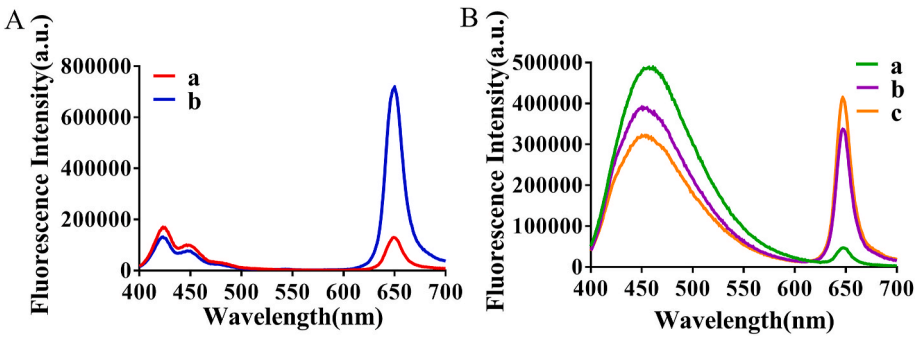

Fig. 1. Feasibility analysis of the L-lactate detection system. The fluorescence spectra of sensing system with different conditions. (A) Pure Pdots-Pt solution. a, Pdots-Pt (2 mg L^{-1}) without blowing nitrogen. b, Pdots-Pt (2 mg L^{-1}) blowing nitrogen. (B) Pdots-Pt applied to L-lactate detection system. a, Pdots-Pt (2 mg L^{-1}) + NADH (0.5 mM) + Lox (7 U mL^{-1}) + LDH (32 U mL^{-1}). b, Pdots-Pt (2 mg L^{-1}) + NADH (0.5 mM) + + pyruvate (0.5 mM) + Lox (7 U mL^{-1}) + LDH (32 U mL^{-1}). c, Pdots-Pt (2 mg L^{-1}) + NADH (0.5 mM) + L-lactate (0.5 mM) + Lox (7 U mL^{-1}) + LDH (32 U mL^{-1}).

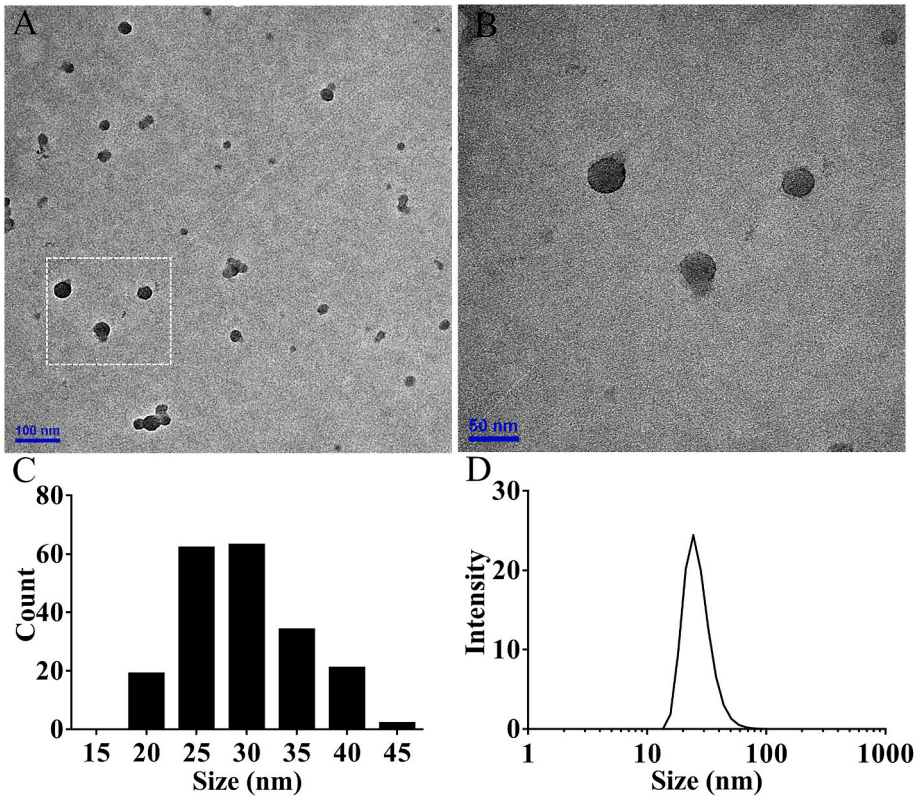

Fig. 2. Characterization of Pdots-Pt. TEM characterization of Pdots-Pt (A) scale = 100 nm, (B) scale = 60 nm, and (C) size distribution. (D) Hydrodynamic diameters of Pdots-Pt.

enhanced with time, which reached a plateau after 30 min. Therefore, 30 min was chosen as the optimal reaction time for the following investigations. Furthermore, the fluorescence background and response depended on the concentration of Pdots-Pt which was also optimized to obtain the best signal to noise (S/N) ratio. Because the amount of oxygen in the solution was constant, the normalized fluorescence intensity did not continue to increase even if there were excess Pdots-Pt in the system. As exhibited in Fig. 3C, the highest S/N ratio was achieved when the concentration of Pdots-Pt was 5 mg L^{-1}, which was used in the following experiments.

The enzyme played key roles in this sensor system. The concentration and efficiency of the two enzymes in the system would affect the final ratiometric fluorescence intensities. Therefore, the pH was optimized to obtain the best normalized fluorescence ratio (Fig. 3D). The results showed that both enzymes had good performance in the system with pH 5.5–9.5, indicating that the system had good stability. Herein, we chose pH 7.5 as the optimal pH for the following experiments because it showed the highest S/N ratio. Apart from that, the impacts of the concentration of LDH and Lox on the biosensor were also investigated. As shown in Fig. 3E, the fluorescence intensity at 650 nm increased gradually when the concentration of Lox increased from 0 U mL^{-1} to 7.0 U mL^{-1} and stayed unchanged thereafter. Thus, 7.0 U mL^{-1} Lox was the optimal concentration used in the sensing system. The results showed that S/N ratio reached the highest value when the concentration of LDH was 32 U mL^{-1} (Fig. 3F). After 32 U mL^{-1}, the reaction efficiency of LDH decreased, which might be due to the pyruvate reduction being too fast, so the newly generated L-lactate was hard to diffuse and proceed to the next round of lactate oxidation with Lox. Therefore, the optimal

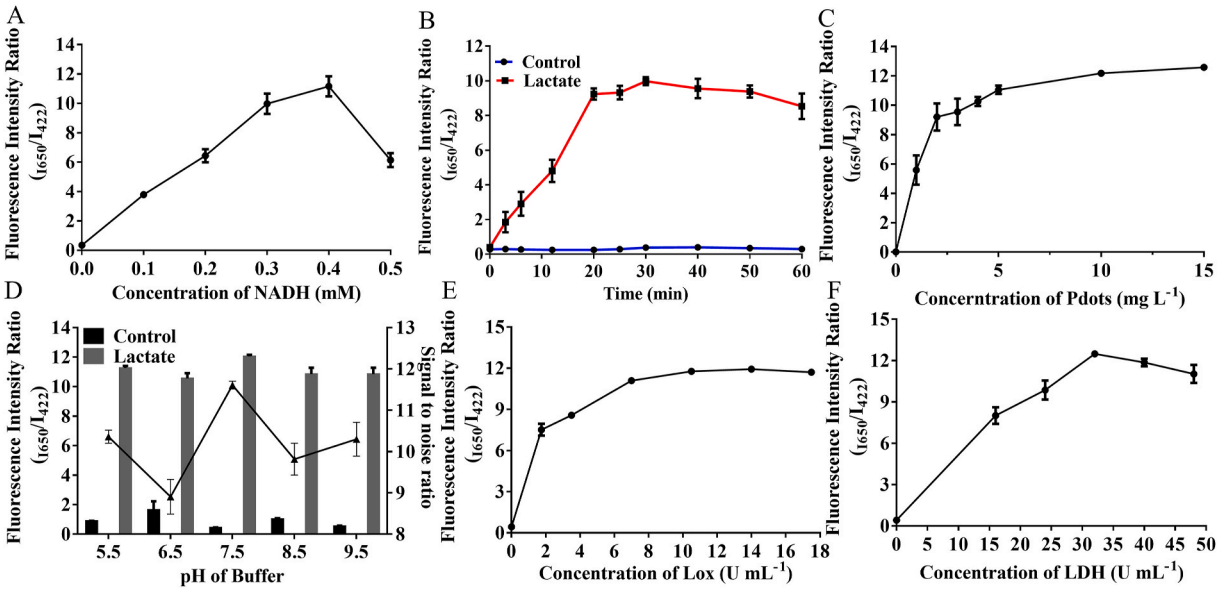

Fig. 3. Optimization of the lactate detection system. (A) Optimization of the concentration of NADH. (B) The effect of reaction time on the fluorescence intensity. (C) The effect of the concentration of Pdots-Pt on the fluorescence intensity of system. (D) The effect of pH on the fluorescence intensity. (E) The effect of the amount of Lox on the fluorescence intensity. (F) The effect of the amount of LDH on the fluorescence intensity.

concentration of LDH was fixed at 32 U mL^{-1} in the following experiments. Since enzymes are temperature sensitive, we also examined the effect of temperature on the detection system. The optimal reaction temperature of Lox is 37 °C, and the optimal reaction temperature of LDH is 25 °C, so we tested the analytical performance of the detection system at room temperature (20 °C), 25 °C and 37 °C (Fig. S2). The results show that at three different reaction temperatures showed high S/N ratio with no significant difference. Controlling the reaction temperature will make the detection operation more complicated, so we chose room temperature as the reaction temperature for subsequent experiments.

3.5. Analytical performance of the lactate detection system

In order to evaluate the analytical performance of the sensing system for lactate detection, the dynamic range and sensitivity of the sensing system for lactate was investigated under the optimized conditions. The results in Fig. 4A showed the fluorescence spectra of the sensing system

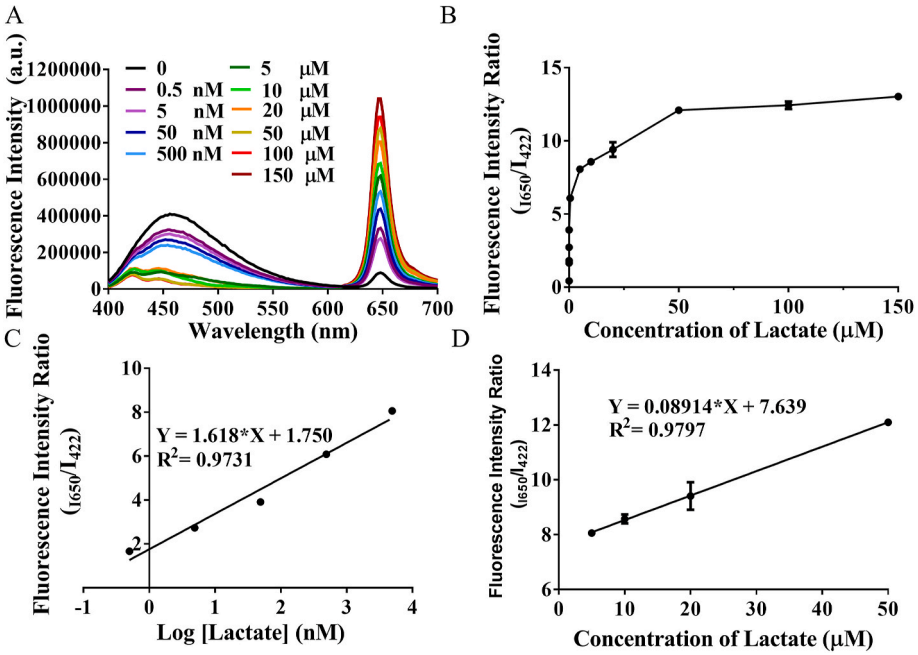

Fig. 4. Sensitivity of the lactate detection system. (A) Fluorescence spectra of sensor system which the concentration of target is increasing from 0.5 nM to 150 μM. (B) The fluorescence intensity ratio (I_{650}/I_{422}) of target with different concentration between 0.5 nM–150 μM. (C) Correlation analysis between fluorescence intensity ratio (I_{650}/I_{422}) and different logarithmic concentrations of lactate between 0.5 nM–5 μM. (D) Correlation analysis between fluorescence intensity ratio (I_{650}/I_{422}) and different concentrations of lactate between 5 μM–50 μM.

with the addition of the different concentrations of lactate. The results demonstrated that the red fluorescence at 650 nm was gradually enhanced and the blue with fluorescence around 422 nm was gradually decreased with the increased concentration of lactate, indicating that more O_2 and NADH were consumed after the enzymatic cascade reaction. The calibration curve of the sensing system towards the concentration of lactate was demonstrated in Fig. 4B–D. The system showed two linear ranges, including 0.5 nM to 0.5 μM and 0.5 μM–50.0 μM. When lactate concentration was between 0.5 nM and 0.5 μM, the normalized fluorescence intensity would have a good linear relationship with the logarithm of concentration of lactate, the regression equation was $Y = 1.618X + 1.750$ with a correlation coefficient of 0.9731 (Fig. 4C). Y represented as fluorescence intensity ratio between 650 nm and 422 nm and X represented as the logarithm of concentration of lactate. In the other hand, when lactate concertation increased from 0.5 μM to 50.0 μM, the normalized fluorescence intensity would have a good linear relationship with the concentration of lactate, the regression equation was $Y = 0.08914X + 7.639$ with a correlation coefficient of 0.9797 (Fig. 4D). Y represented as fluorescence intensity ratio between 650 nm and 422 nm and X represented as the concentration of lactate. The reason for the existence of two linear relationships is that the dominant enzyme-mediated reaction is different when the lactate concentration is changed. When lactate was in trace amounts, since the concentration of LDH was more than 4 times that of Lox, LDH-mediated pyruvate reduction was the key step. At this stage, the main influence on the normalized fluorescence signal is the consumption of NADH. However, when lactate was in large amounts, Lox-mediated lactate oxidation was predominant. At this stage, the main influence on the normalized fluorescence signal is the consumption of O_2. Also, when lactate existed in large amounts, the enzymatic reaction exhibited first-order kinetics, resulting in that the lactate concentration had a linear relationship with the normalized fluorescence. However, when only trace amounts of lactate are present, the signal was amplified primarily through an enzymatic cascade reaction, where the lactate concentration had a logarithmic relationship with the normalized fluorescence [36,37]. The limit of detection (LOD) was calculated to be 0.18 nM according to the 3σ/slope rule from linear range between 0.5 and 5000 nM. This result is comparable to or even better than the reported method of lactate detection (Table 1) [[38–46]].

Table 1
Comparison the analytical performances between the reported papers and this work.

Methods	LOD (μM)	Linear range (μM)	Ref
Amperometry (Pt/PANI/MXene)	1	5–5000	[44]
Amperometric (Au planar electrode with Au nanoclusters)	100	300–2000	[45]
Potentiometric (RGO-Au nanoparticles)	0.13	10–5000	[38]
Colorimetry (Au–Ag/C NC)	0.033	0.1–220	[46]
Fluorometric (ZnO NWs)	0.24	Up to 1.1	[39]
Electrochemistry (Indium tin oxide electrode, modified with a graphene-like membrane)	0.165	0.55–3330	[41]
Electrochemistry ((Flexible graphene oxide)	1000	1000–100000	[42]
Fluorometric (Amorphous metal−organic frameworks)	0.3	2–80	[47]
Electrochemistry (laser-scribed graphitic carbon modified with platinum, chitosan and lactate oxidase)	110	200–3000	[13]
Electrochemistry (Hierarchical gold dispersed nickel oxide nanodendrites microarrays)	0.1	10–5000	[48]
HPLC	5.24	10–200	[40]
Ratiometric fluorescence (bCDs/AgNPs-rQDs)	0.12	0.05–100	[43]
Ratiometric fluorescence with the help of enzymatic cascade reaction (Pdots-Pt)	0.00018	0.0005–5	This work

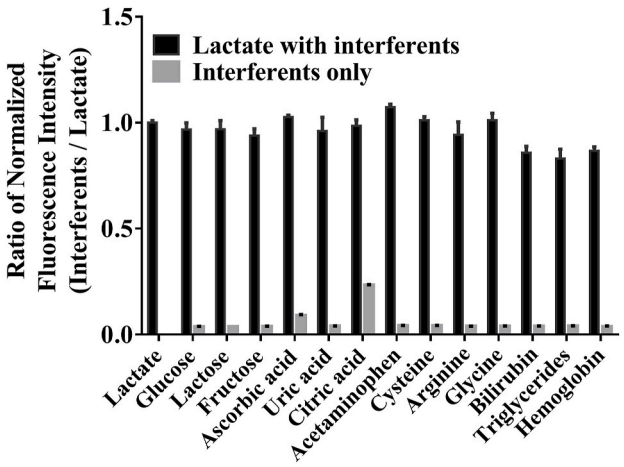

Fig. 5. Selectivity of lactate detection. The normalized fluorescence intensity of target and target with interferents or interferents only, with the concentrations of lactate and lactate with interferents were 0.5 mM and 0.5 + 0.5 mM, and interferents (0.5 mM), respectively.

Next, the selectivity of the sensing system was investigated with different nonspecific interferences. As shown in Fig. 5, when the nonspecific interferents (0.5 μM) was mixed with or without lactate (0.5 μM), the interferents (carbohydrate, organic acids, electroactive substances, amino acid, bilirubin, triglycerides, hemoglobin) did not affect the detection of lactate. Since Pdots-Pt has an abundant carboxyl group on its surface, which can lead to sensitivity to metal ions. Therefore, the selectivity of the sensing system was investigated with different metal ions including Zn^{2+}, Li^{+}, Cu^{2+}, Ca^{2+}, Mg^{2+}, Fe^{3+}, and Fe^{2+}, and the metal ions did not affect the detection of L-lactate (Fig. S3). The high selectivity was due to the factor that the Lox and LDH had high catalytic selectivity to lactate and pyruvic, respectively. These results exhibited that the designed sensing system could provide excellent sensitivity and selectivity for lactate detection. We also tested the stability and repeatability of the detection system. As shown in Fig. S4A, the sensing system obtained consistent results for the detection of lactate with same concentration for 7 days, indicating that the detection system had good stability. On the other hand, as shown in Fig. S4B, when different batches of detection systems were prepared using the same experimental protocol, similar results were achieved for the measurement of lactate, indicating that the probe and detection system had good repeatability. However, one of the limitations is that the normal L-lactate value in blood is on the level of milli-molar range. In order to precisely detect the L-lactate concentration in blood sample, a dilution step is required for our sensor for real blood sample measurement.

3.6. Real sample analysis

In order to verify the analytical performance of the sensing system under complex conditions, we carried out standard recovery experiments to evaluate the sensing system in diluted fetal bovine serum (FBS) samples. In clinical blood samples, the concentration of lactate in blood is about 0.5–1.7 mM under normal conditions. In hyperlactatemia, the concentration of lactate in blood can be higher than 2.5 mM without metabolic acidosis. L-lactate poisoning refers to the condition that the concentration of lactate in blood reaches 5 mM accompanied by metabolic acidosis, which causing several physiological disturbances. The remarkably low detection limit of our method enabled the identification of even trace amounts of L-lactate. In practical applications, the low detection limit indicated that only a small amount of blood sample is required for the detection. We choose four concentrations of L-lactate (20.0 nM, 200.0 nM, 10.0 μM and 40.0 μM) spiked into the 5% diluted FBS to investigate the recovery which represent real sample been dilute

Table 2
Determination of lactate in fetal bovine serum samples.

Sample	Spiked	Recovery (%)	RSD (%)
Serum	20.00 nM	109.6	0.3
	200.00 nM	105.8	4.1
	10.00 μM	118.8	2.5
	40.00 μM	96.8	0.06

Table 3
Determination of lactate in artificial serum samples.

Method	Lactate concentration	Recovery (%)	RSD (%)
Lactate Assay Kit	2.00 mM	98.6	10.0
	0.50 mM	103.4	6.0
This method	2.00 mM	96.7	3.0
	0.50 mM	96.3	5.4

for 10,000 times (0.2 mM and 2 mM) or 100 times (1 mM and 4 mM). Four concentrations of lactate (20.0 nM, 200.0 nM, 10.0 μM and 40.0 μM) were spiked into the 5% diluted FBS to investigate the recovery. The results in Table 2 showed that the recoveries were 109.6%, 105.8%, 118.8% and 96.8 %, respectively for these four concentrations which is referenced against prepared solutions. The relative standard derivations (RSD) were 0.3%, 4.1%, 2.5% and 0.06 %, respectively. Moreover, we investigated two artificial serum samples containing 2 mM and 0.5 mM L-lactate respectively, to simulate serum compositions representative of human disease states and normal physiological conditions. As shown in Table 3, the standard commercial kit for lactate demonstrated recovery rates of 98.6% and 103.4% for those two different concentrations. Our methods showed recovery rates of 96.7% and 96.3%, respectively. Both methods achieved low RSD. Our method exhibited lower RSD (3.0% and 5.4%) compared with the standard kit (10.0% and 6.0%). These results indicated that the developed sensing system could be used for the lactate detection in complex biological samples. These results indicated that the developed sensing system could provide applications in complex biological samples.

4. Conclusion

In conclusion, we developed a simple and sensitive detection method for L-lactate analysis based on cyclic amplification by enzymatic cascade reaction and bright Pdots-Pt. In the proposed method, the NADH and oxygen in the system induced bright initial blue fluorescence from NADH and weak red fluorescence from Pdots-Pt, respectively. Once L-lactate was present, Lox efficiently converted L-lactate to pyruvate, while consuming oxygen. Then, LDH catalyzed the produced pyruvate back to L-lactate, consuming NADH. Once the oxygen or NADH in the system was exhausted, the reaction stopped, resulting in enhanced red fluorescence and reduced blue fluorescence. Under the optimized conditions, the sensing system not only showed excellent selectivity to the L-lactate, but also had two linear detection ranges from 0.5 nM to 5.0 μM and 5.0 μM–50.0 μM, with LOD of 0.18 nM. Moreover, the sensing system showed excellent selectivity to different types of interferences. With such low detection limit and lower linear dynamic range of the sensing system, it is required a dilution step for the detection of L-lactate in the real blood sample, but at the same time, small amount of blood will be needed for the developed method. Meanwhile, the successful application of the sensing system in the complex biological sample (diluted serum and artificial serum sample) clearly demonstrated that this method could be used for sensitive L-lactate detection in practical clinical settings, which may provide a useful method for L-lactate monitoring to predict the related diseases such as hypoxia and respiratory failure. In the future, we will focus on the integration of our proposed method into a portable device that has the potential to be used for rapid detection of L-lactate.

CRediT authorship contribution statement

Shuyi He: Data curation, Formal analysis, Software, Writing – original draft, Writing – review & editing. **Weichao Liu:** Software. **Steven Xu Wu:** Funding acquisition, Supervision.

Declaration of competing interest

The authors declare that they have no known competing financial interests or personal relationships that could have appeared to influence the work reported in this paper.

Data availability

Data will be made available on request.

Acknowledgment

S.X.W. acknowledges the start-up package supported by the University of South Dakota, National Institute of General Medical Sciences of the National Institutes of Health under Award Number U54GM128729, and NSF award 2316812.

Appendix A. Supplementary data

Supplementary data to this article can be found online at https://doi.org/10.1016/j.aca.2024.342523.

References

[1] G. Rattu, N. Khansili, V.K. Maurya, Lactate detection sensors for food, clinical and biological applications: a review, Environ. Chem. Lett. 19 (2021) 1135–1152.
[2] Z. Zhang, X. Xu, Lactate clearance is a useful biomarker for the prediction of all-cause mortality in critically ill patients: a systematic review and meta-analysis, Crit. Care Med. 42 (2014) 2118–2125.
[3] L. Rassaei, W. Olthuis, S. Tsujimura, Lactate biosensors: current status and outlook, Anal. Bioanal. Chem. 406 (2014) 123–137.
[4] W.A. Neill, P.E. Jensen, G.B. Rich, Effect of decreased o2 supply to tissue on the lactate: pyruvate ratio in blood, J. Clin. Invest. 48 (1969) 1862–1869.
[5] N. Nikolaus, B. Strehlitz, Amperometric lactate biosensors and their application in (sports) medicine, for life quality and wellbeing, Microchim. Acta 160 (2008) 15–55.
[6] J.B. Ewaschuk, G.A. Zello, J.M. Naylor, Metabolic acidosis: separation methods and biological relevance of organic acids and lactic acid enantiomers, J. Chromatogr. B 781 (2002) 39–56.
[7] K. Nagamine, T. Mano, R. Shiwaku, An l-lactate biosensor based on printed organic inverter circuitry and with a tunable detection limit, Sensor. Mater. 31 (2019) 1205.
[8] R. Wijngaard, M. Perramón, M. Parra-Robert, Validation of a gas chromatography-mass spectrometry method for the measurement of the redox state metabolic ratios lactate/pyruvate and β-hydroxybutyrate/acetoacetate in biological samples, Int. J. Mol. Sci. 22 (2021).
[9] A. Bertaso, E.F. De Palo, V. Cirielli, Lactate determination in human vitreous humour by capillary electrophoresis and time of death investigation, Electrophoresis (Weinheim, Fed. Repub. Ger.) 41 (2020) 1039–1044.
[10] C.L. Hsieh, R. Koga, A. Furusho, Enantioselective and simultaneous determination of lactate and 3-hydroxybutyrate in human plasma and urine using a narrow-bore online two-dimensional high-performance liquid chromatography system, J. Separ. Sci. 41 (2018) 1298–1306.
[11] Xu X, Xu R, Hou S, A selective fluorescent l-lactate biosensor based on an l-lactate-specific transcription regulator and förster resonance energy transfer, Biosensors 12 (2022) 1111.
[12] A. Golparvar, J. Kim, A. Boukhayma, Highly accurate multimodal monitoring of lactate and urea in sweat by soft epidermal optofluidics with single-band Raman scattering, Sensor. Actuator. B Chem. 387 (2023) 133814.
[13] J. Madden, E. Vaughan, M. Thompson, Electrochemical sensor for enzymatic lactate detection based on laser-scribed graphitic carbon modified with platinum, chitosan and lactate oxidase, Talanta 246 (2022) 123492.
[14] W. Shi, J. Wang, L. Zhu, Electrochemical determination of catechin, protocatechuic acid, and l-lactic acid based on voltammetric response of ferroceneboronic acid, J. AOAC Int. 97 (2014) 1742–1745.
[15] A. Zhou, J. Ni, Z. Xu, Metabolomics specificity of tuberculosis plasma revealed by (1)h nmr spectroscopy, Tuberculosis 95 (2015) 294–302.
[16] N. Gajovic, G. Binyamin, A. Warsinke, Operation of a miniature redox hydrogel-based pyruvate sensor in undiluted deoxygenated calf serum, Anal. Chem. 72 (2000) 2963–2968.

[17] A. Bigdeli, F. Ghasemi, S. Abbasi-Moayed, Ratiometric fluorescent nanoprobes for visual detection: design principles and recent advances - a review, Anal. Chim. Acta 1079 (2019) 30–58.
[18] R. Gui, H. Jin, X. Bu, Recent advances in dual-emission ratiometric fluorescence probes for chemo/biosensing and bioimaging of biomarkers, Coord. Chem. Rev. 383 (2019) 82–103.
[19] Y. Cui, F. Chen, X.B. Yin, A ratiometric fluorescence platform based on boric-acid-functional eu-mof for sensitive detection of h(2)o(2) and glucose, Biosens. Bioelectron. 135 (2019) 208–215.
[20] W. Xiao, F. Liu, G.-P. Yan, Yttrium vanadates based ratiometric fluorescence probe for alkaline phosphatase activity sensing, Colloids Surf., B 185 (2020) 110618.
[21] M.H. Lee, J.S. Kim, J.L. Sessler, Small molecule-based ratiometric fluorescence probes for cations, anions, and biomolecules, Chem. Soc. Rev. 44 (2015) 4185–4191.
[22] S.-H. Park, N. Kwon, J.-H. Lee, Synthetic ratiometric fluorescent probes for detection of ions, Chem. Soc. Rev. 49 (2020) 143–179.
[23] C. Duan, M. Won, P. Verwilst, In vivo imaging of endogenously produced hclo in zebrafish and mice using a bright, photostable ratiometric fluorescent probe, Anal. Chem. 91 (2019) 4172–4178.
[24] M.-J. Cho, S.-Y. Park, Carbon-dot-based ratiometric fluorescence glucose biosensor, Sensor. Actuator. B Chem. 282 (2019) 719–729.
[25] C. Wu, D.T. Chiu, Highly fluorescent semiconducting polymer dots for biology and medicine, Angew. Chem. Int. Ed. 52 (2013) 3086–3109.
[26] W. Hou, Y. Yuan, Z. Sun, Ratiometric fluorescent detection of intracellular singlet oxygen by semiconducting polymer dots, Anal. Chem. 90 (2018) 14629–14634.
[27] X. Bai, K. Wang, L. Chen, Semiconducting polymer dots as fluorescent probes for in vitro biosensing, J. Mater. Chem. B 10 (2022) 6248–6262.
[28] X.-M. Shi, L.-P. Mei, N. Zhang, A polymer dots-based photoelectrochemical ph sensor: simplicity, high sensitivity, and broad-range ph measurement, Anal. Chem. 90 (2018) 8300–8303.
[29] N. Alizadeh, A. Salimi, Polymer dots as a novel probe for fluorescence sensing of dopamine and imaging in single living cell using droplet microfluidic platform, Anal. Chim. Acta 1091 (2019) 40–49.
[30] M. Verma, Y.-H. Chan, S. Saha, Recent developments in semiconducting polymer dots for analytical detection and nir-ii fluorescence imaging, ACS Appl. Bio Mater. 4 (2021) 2142–2159.
[31] S. Wang, M. Huang, J. Hua, Digital counting of single semiconducting polymer nanoparticles for the detection of alkaline phosphatase, Nanoscale 13 (2021) 4946–4955.
[32] C. Wu, B. Bull, K. Christensen, Ratiometric single-nanoparticle oxygen sensors for biological imaging, Angew. Chem. Int. Ed. 48 (2009) 2741–2745.
[33] E.T. Hwang, S. Lee, Multienzymatic cascade reactions via enzyme complex by immobilization, ACS Catal. 9 (2019) 4402–4425.
[34] Q. Qu, X. Zhang, H. Ravanbakhsh, Gas-shearing synthesis of core–shell multicompartmental microparticles as cell-like system for enzymatic cascade reaction, Chem. Eng. J. 428 (2022) 132607.
[35] K. Sun, Z. Ding, J. Zhang, Enhancing the long-term stability of a polymer dot glucose transducer by using an enzymatic cascade reaction system, Adv. Healthcare Mater. 10 (2021) 2001019.
[36] Z. Zhang, L. Zhang, Y. Wang, Ultrasensitive electrochemical biosensor for attomolar level detection of let 7a based on toehold mediated strand displacement reaction circuits and molecular beacon mediated circular strand displacement polymerization, Anal. Chim. Acta 1147 (2021) 108–115.
[37] W.W. Chen, B. Schoeberl, P.J. Jasper, Input–output behavior of erbb signaling pathways as revealed by a mass action model trained against dynamic data, Mol. Syst. Biol. 5 (2009) 239.
[38] S. Azzouzi, L. Rotariu, A.M. Benito, A novel amperometric biosensor based on gold nanoparticles anchored on reduced graphene oxide for sensitive detection of l-lactate tumor biomarker, Biosens. Bioelectron. 69 (2015) 280–286.
[39] M. Briones, C. Busó-Rogero, S. Catalán-Gómez, Zno nanowire-based fluorometric enzymatic assays for lactate and cholesterol, Mikrochim. Acta 187 (2020) 180.
[40] G. Cevasco, A.M. Piątek, C. Scapolla, A simple, sensitive and efficient assay for the determination of d- and l-lactic acid enantiomers in human plasma by high-performance liquid chromatography, J. Chromatogr., A 1218 (2011) 787–792.
[41] H. Cheng, C. Hu, Z. Ji, A solid ionic lactate biosensor using doped graphene-like membrane of au-evimc-titania nanotubes-polyaniline, Biosens. Bioelectron. 118 (2018) 97–101.
[42] K.-C. Lin, S. Muthukumar, S. Prasad, Flex-go (flexible graphene oxide) sensor for electrochemical monitoring lactate in low-volume passive perspired human sweat, Talanta 214 (2020) 120810.
[43] Y. Ma, Y. Wang, Y. Liu, A cascade-triggered ratiometric fluorescent sensor based on nanocomposite for lactate determination, Sensor. Actuator. B Chem. 355 (2022) 131295.
[44] S. Neampet, N. Ruecha, J. Qin, A nanocomposite prepared from platinum particles, polyaniline and a ti(3)c(2) mxene for amperometric sensing of hydrogen peroxide and lactate, Mikrochim. Acta 186 (2019) 752.
[45] O. Smutok, M. Karkovska, R. Serkiz, A novel mediatorless biosensor based on flavocytochrome b2 immobilized onto gold nanoclusters for non-invasive l-lactate analysis of human liquids, Sensor. Actuator. B Chem. 250 (2017) 469–475.
[46] L. Zhang, W. Hou, Q. Lu, Colorimetric detection of hydrogen peroxide and lactate based on the etching of the carbon based au-ag bimetallic nanocomposite synthesized by carbon dots as the reductant and stabilizer, Anal. Chim. Acta 947 (2016) 23–31.
[47] Y. Zhang, L. Xu, J. Ge, Multienzyme system in amorphous metal–organic frameworks for intracellular lactate detection, Nano Lett. 22 (2022) 5029–5036.
[48] M. Arivazhagan, G. Maduraiveeran, Hierarchical gold dispersed nickel oxide nanodendrites microarrays as a potential platform for the sensitive electrochemical detection of glucose and lactate in human serum and urine, Mater. Chem. Phys. 295 (2023) 127084.